Paper ID: 438

Aerodynamic Performance Analysis of a Biomimetic based Fixed Wing for Micro Aerial Vehicle Applications

Md. Hasibul Hasan Himel[1*], Mohammad Raihan[1], Md. Kobir Hossain Mrida[1], Fardeen Sayed[2], Mim Mashrur Ahmed[1], Md. Rokunuzzaman[1]
[1]Department of Mechanical Engineering, Rajshahi University of Engineering & Technology, Rajshahi-6204, Bangladesh
[2]Department of Mechanical and Production Engineering, Ahsanullah University of Science and Technology, Dhaka-1208, Bangladesh
Email: [1,]hasibul.hasan@me.ruet.ac.bd*

Abstract

Micro Aerial Vehicles (MAVs) operate at low Reynolds number ranging from 10^4-10^5 and flows with low Reynolds number experience phenomena like laminar separation bubble which results in an early stall. In order to effectively implement any wing for MAVs, it is crucial to get a thorough understanding of the essential aerodynamic properties such as lift coefficient (C_L) and drag coefficient (C_d). An appropriate first step would include examining the aerodynamic characteristics of a wing in order to assess its suitability for incorporation into the design configuration of a MAV. This study investigates the effect of the Humpback whale inspired leading edge tubercles on the performance of a fixed wing MAV. The wing profile of this fixed wing MAV is generated from S5010, and numerical investigations are carried out at Reynolds number 1×10^5. The wing shape maintains an aspect ratio of 1.5, while the tubercles' amplitude and wavelength are kept at 0.5 cm and 4.29 cm, respectively. The numerical analysis showed that the tubercle model provides higher lift coefficients, lower drag coefficients and higher lift-to-drag coefficients compared to the baseline model. The maximum lift coefficient was recorded as 0.93 at 20° angle of attack (AoA) and the maximum lift-to-drag ratio was noted as 9 at 10° AoA for the tubercle model. This study reveals that incorporation of tubercle blade in MAV application will allow its operation at wide range of AoA and ensure better aerodynamic performance at higher AoAs compared to the MAV with conventional S5010 airfoil.

Keywords: MAV, biomimetic wing, lift coefficient, drag coefficient, aerodynamic performance.

1. Introduction

Over the last two decades, the fast advancement of new technologies has resulted in more compact electronic equipment (e.g., motors, sensors, miniaturized control systems), thus facilitating the quick evolution of radio-controlled unmanned aerial vehicles (UAV). Micro air vehicles (MAVs), characterized as a category of unmanned aircraft with a maximum size of 15 cm and a flying speed under 15 m/s, draw growing interest due to its prospective military and commercial uses [1]. The principal objectives of micro air vehicles are surveillance, detection, communication, and rescue operations. There are three classifications of MAVs: fixed-wing, rotary-wing, and flapping-wing kinds. Fixed-wing models resemble conventional aircraft, exhibit high efficiency, and possess prolonged flying durations [2]. Fixed-wing MAVs are often preferred for extended-duration, long-range missions necessitating loitering and surveillance. Despite their superior speed compared to other designs, their maneuverability is poor, particularly in proximity to buildings, trees, or other obstacles. However, the small size and reduced flying velocity cause MAVs to function within a low Reynolds number domain (usually 10^4–10^5), far lower than that of conventional aircraft [1]. Research indicates that the aerodynamic efficiency of a streamlined airfoil designed for conventional macroscale aircraft at high Reynolds numbers drastically deteriorates when the Reynolds number is decreased [3]. Therefore, MAVs with traditional streamlined airfoil designs often exhibit suboptimal aerodynamic performance, hence limiting their flying agility and adaptability. Moreover, an adverse flow characteristic in low Reynolds number airfoil aerodynamics is the occurrence of a laminar separation bubble

on the suction surface of the airfoil, which increases drag and therefore reduces the lift-to-drag ratio [1]. It is observed that when traditional NACA airfoil has been used for fixed wing MAVs, it results in early stall and decreased aerodynamic efficiency [4]. Consequently, it is essential to develop innovative airfoil design paradigms for MAV applications to enhance aerodynamic performance, thus improving flying agility and adaptability. Bio-inspired wing design for fixed wing MAVs can be a better alternative in that case. Biological species have extremely advantageous traits in their natural behaviors in both aquatic and aerial environments, which can enhance the performance of MAVs if properly replicated. Although several studies have been undertaken on the biomimetic approach of flapping wing MAVs [5], the incorporation of biomimetic features in fixed-wing MAVs remains insufficient. Among various biological species, the leading-edge tubercles derived from Humpback whale flippers provide significant potential to enhance the aerodynamic efficiency of fixed wing MAVs by improving wing maneuverability [6]. Despite the multiple aerodynamic advantages of Humpback whale flippers [7], the primary traits influencing their selection as inspiration for biomimetic fixed-wing MAV design are the phenomena of stall delay and enhanced flow control at high angles of attack. Various researchers investigated the effect of leading-edge tubercles in numerous NACA profiles both numerically and experimentally. A Large Eddy Simulation (LES) conducted by Skillen et al. has shown that an undulated leading edge of the NACA 0021 airfoil results in a 36% increase in mean lift and a 25% decrease in mean drag at a Reynolds number of 1.2×10^5 [8]. Alessandro et al. emphasized the impact of a sinusoidal leading edge applied to NACA 0015 and NACA 4415 airfoil profiles, noting that the asymmetric (cambered) modified airfoil exhibits quicker recovery during stall circumstances and provides a 30% increase in lift during post-stall scenarios [9]. Kim et al. examined the alterations in flow structure caused by leading-edge protuberances on a three-dimensional wing at a Reynolds number of 1.8×10^5. The stall angle is delayed by 7° and C_L max has been raised by 22% for the NACA0020 tubercle model [10]. As MAVs operate at low Reynolds number region, it requires design MAVs with low Reynolds number airfoils having low aspect ratio which is missing in literature. This study has numerically investigated the aerodynamic performance of a biomimetic fixed wing inspired from Humpback whale leading edge tubercles adapted in low Reynolds number aerofoil for application of MAVs. Moreover, a comparative analysis has been presented between the tubercle wing (tubercle model) and wing without tubercle (baseline model).

2. Methodology

The research features two wing models for fixed wing MAV: one wing having no modification (baseline model) and the other inspired by the tubercles of a Humpback Whale flipper, integrated into the leading edge of the baseline model (tubercle model). The geometric characteristics for the wing designed for the application of fixed wing MAV are delineated in **Table 1.** The geometries of the baseline model and the tubercle model were created using SolidWorks 2023 software, as seen in **Fig. 1.**

Table 1: Geometric parameters of wing for fixed wing MAV design.

Parameter	Baseline model	Tubercle model
Airfoil	S5010	S5010
Planform	Rectangular	Rectangular
Equation of wing	N/A	Y=0.5*Sin (1.466*X)
Wing wavelength ($\boldsymbol{\lambda}$)	N/A	4.29 cm
Amplitude (a)	N/A	0.5 cm
Wingspan (s)	15 cm	
Chord length (c)	10 cm	
Wing aspect ratio (AR)	1.5 cm	



(a) (b)

Fig. 1. (a) Baseline model and (b) Tubercle model.

The computational domain utilized in this simulation is identical for the two geometries, as the chord's length remains constant. The computational domain dimensions for the simulation were established in ANSYS Design Modeler as 30C×10C×10C (length×height×depth), where C denotes the chord length. In order to alleviate the instabilities that arise from the outflow boundary, the inflow and outflow boundaries were positioned 10C ahead and 20C behind of the wing geometry, respectively. Moreover, the wing was precisely positioned in the center of the computational domain in relation to its height, as illustrated in **Fig. 2**. In order to generate the highest quality mesh surrounding the geometries, two phases of the "Body of Influence" were implemented within the domain. Dimension of the body of influence has been also shown in **Fig. 2**.

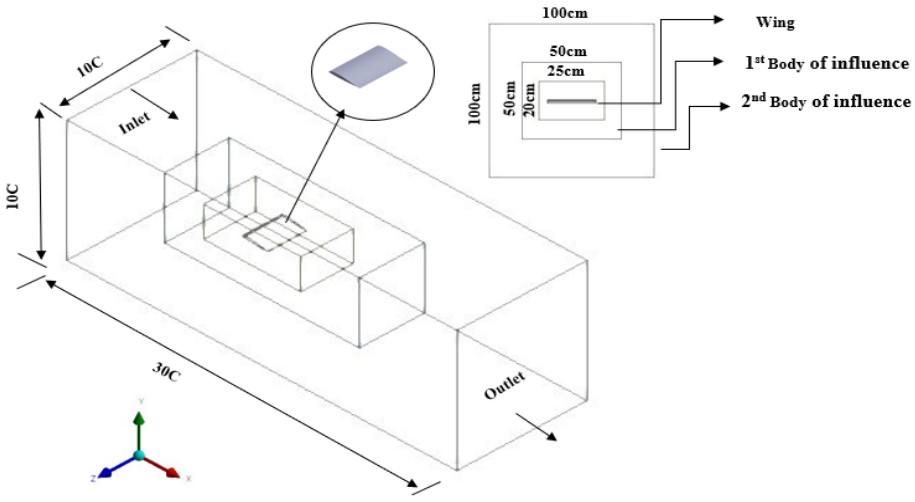


Fig. 2. Isometric view of computational domain.

The mesh used in conclusive study is represented in **Fig. 3**. The quality measurements of this mesh include a maximum orthogonal quality of 0.99 and a skewness of 0.91. The numerical study used a steady k-ω SST (shear-stress transport) model to examine the fluid flow characteristics over the model in ANSYS Fluent software. To accurately get the findings for boundary layer development and separation, 15 inflation layers with a thickness of 1.8×10^{-5} m and a Y+ value of 1 were established for the simulation. All simulations were conducted with an input velocity of 15 m/s, and the chord-based Reynolds number (Re) was 100,000. The Reynolds number was calculated using the methodology outlined in Masud et al. [11]. Additionally, the boundary conditions and other essential characteristics of this investigation are shown in **Table 2**. For getting the most effective mesh size, a mesh sensitivity analysis is performed, by varying the size of the mesh body. The range of mesh element counts varies from 26,383 to 28,69,085 elements. The measured characteristics include the coefficient of lift (C_L) and the coefficient of drag (C_D). It has been shown that the optimal range for element numbers is between 22,00,000 and 30,00,000. The details of the mesh sensitivity analysis are shown in **Fig. 4**. From the results obtained, a total of 28,69,085 elements with small cell size were used for the study.

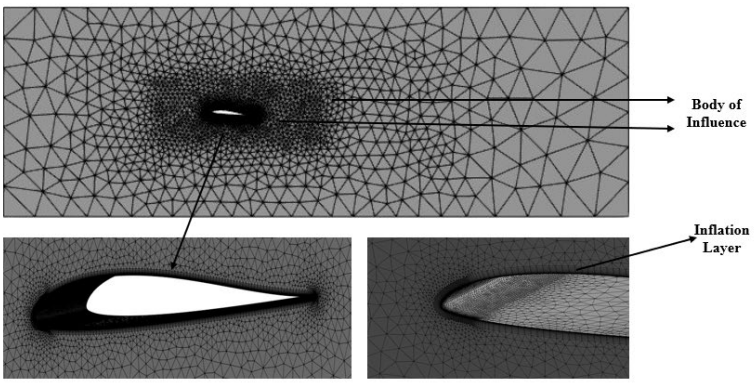
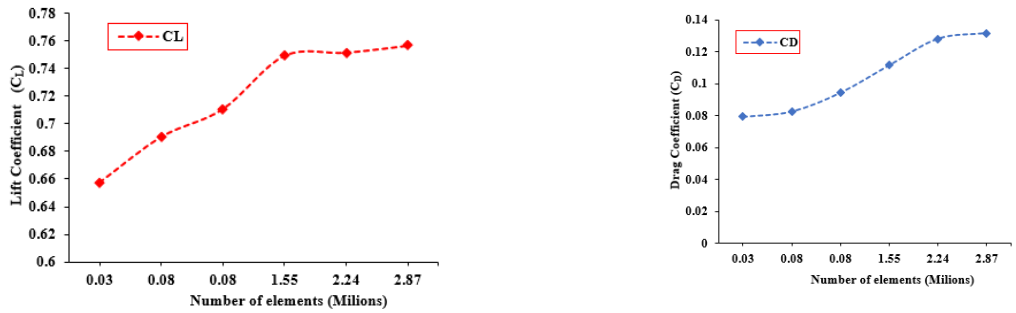


Fig. 3. Mesh generation inside the computational domain.



(a) (b)

Fig. 4. Mesh sensitivity of (a) lift coefficient, (b) drag coefficient with the number of elements (millions) of the baseline models at 15° AoA.

Table 2: Boundary conditions of numerical investigation.

Parameter	Value/type	Parameter	Value/type
Analysis type	Steady	Reference values	Compute from inlet
Viscous model	k-ω model		Area- 0.015 m^2
Fluid velocity	15 m/s		Length- 0.1 m
Reynolds number	1×10^5	Method	Pressure Velocity
Boundary conditions	Inlet-velocity inlet		Couple Scheme
	Outlet-pressure outlet		2^{nd} order
	Wall-no slip		

3. Results and Discussion

The simulations of the study model were conducted using steady state condition. Hence, to verify the obtained results are correct, a research paper[12] has been choosen which focuses on the lift & drag coefficient of a wing with zimmerman planform for various profile. For varifying the simulation procedure, only profile-3 was choosen for the simulation. The results obtained was almost similar to the given values of coefficient of lift & drag. **Fig. 5** illustrates the variation of lift coefficients (C_L), drag coefficients (C_D) and lift-to-drag ratios (C_L/C_D) with the angles of attack (AoA) for both the baseline airfoil and tubercle airfoil. As expected, the tubercle model outperformed the baseline model showing higher lift coefficient, lower drag and higher lift-to-drag ratio. The maximum lift coefficient of the baseline model was 0.90 at 18° AoA and that of the tubercle model was 0.93 at 20° AoA. Hence, the tubercle model will allow the MAVs to be operated at a wider range of AoAs compared to the baseline model. Additionally, although the baseline and tubercle models had almost similar lift coefficients at lower AoAs (≤18°), the lift coefficients of the tubercle model were significantly higher than the baseline model at higher AoAs. Literature also reveals that the tubercle airfoil has the potential to be used at higher AoAs compared to the conventional airfoils [13]. The drag coefficients of the tubercle model were lower in higher AoAs compared to the baseline model indicating that it will offer better fuel efficiency if implemented in aerial vehicle applications. The tubercle model offered approximately similar lift-to-drag ratios at low AoAs (≤5°) but the difference became significantly higher at higher AoAs (≥5°). The maximum lift-to-drag ratio was 9 at 10° AoA and was 8 at 5° AoA for tubercle model and baseline model, respectively.

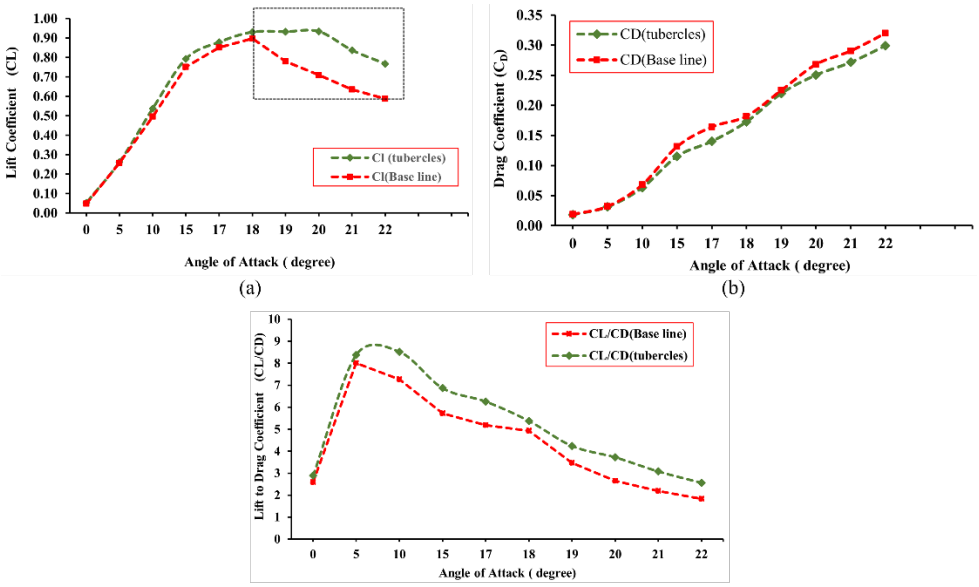


Fig. 5. Variation of (a) lift coefficient, (b) drag coefficient and (c) lift-to-drag ratio with the angle of attack of the baseline and tubercle models.

Fig. 6 presents the pressure and velocity contour plots of the baseline and tubercle models at 15° AoA. Here, 15° AoA is chosen as a representative for all the angles as the pressure and velocity distribution will be identical in terms of appearance for other AoAs. **Fig. 6(a)** reveals that comparatively lower pressure exists on the upper surface of the airfoils than on the lower surface resulting in a lift force in upper direction. Additionally, the pressure difference between the top and bottom face of the tubercle model is higher than that of the baseline model (see **Fig. 6(a)**) which indicates higher lift force for tubercle model at 15° AoA similar to the data shown in **Fig. 4(a)**. Besides, velocity contour in **Fig. 6(b)** reveals that higher velocity exists in the top surface of the airfoil compared to the bottom surface, as the pressure was higher in the top surface, suggesting an upward lift force in the airfoils at 15° AoA. The velocity difference between top and bottom faces is higher for the tubercle model than the baseline one indicating higher lift force in the upward direction.

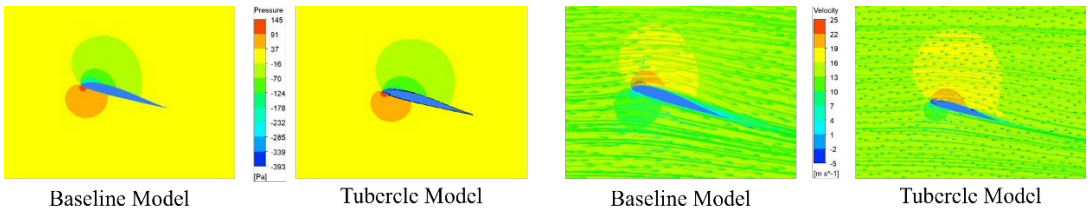


Fig. 6. (a) Pressure contour plot and (b) velocity contour plot of the baseline and tubercle airfoils at 15° AoA.

Fig. 7 presents the wall shear distribution of the airfoils at 15° AoA. More shear stress variation on the airfoil face was observed for the tubercle model compared to the baseline model with a negative pressure in several regions at the leading edge. Velocity distribution around the airfoil face can easily be interpreted from the wall shear distribution. The larger wall shear variation on the tubercle model indicates the generation of turbulent boundary layer due to the presence of tubercles in the blade.

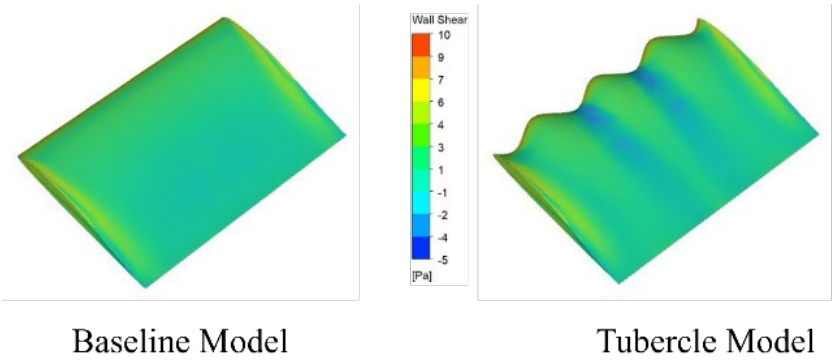


Fig. 7. Wall shear distribution on the baseline and modified blades at 15° AoA.

4. Conclusion

This study demonstrates that incorporating biomimetic features inspired by Humpback whale flippers into the design of fixed-wing MAVs significantly enhances aerodynamic performance. The tubercle model, featuring a sinusoidal leading edge, showed improved lift coefficients, reduced drag, and a higher lift-to-drag ratio compared to the conventional baseline model. The findings indicate that the tubercle model supports operation over a wide range of angles of attack, providing increased maneuverability and stability in low Reynolds number environments, which is critical for MAV applications. These results suggest that biomimetic design approaches hold substantial potential for advancing MAV technology, particularly in applications where agility, energy efficiency, and versatility are paramount.

5. References

[1] T. Xiao, Z. Li, S. Deng, H. Ang, and X. Zhou, "Numerical study on the flow characteristics of micro air vehicle wings at low Reynolds numbers," *International Journal of Micro Air Vehicles*, vol. 8, no. 1, pp. 29–40, Mar. 2016, doi: 10.1177/1756829316638204.

[2] M. H. Masud, "Biomimetic Applications of Penguins' Geometric Features: Feasibility and Performance Analysis," PhD Thesis, RMIT University, 2023. Accessed: Oct. 31, 2024. [Online]. Available: https://researchrepository.rmit.edu.au/view/pdfCoverPage?instCode=61RMIT_INST&filePid=13310060540001341&download=true

[3] B. H. Carmichael, "Low Reynolds number airfoil survey, volume 1," 1981. Accessed: Oct. 31, 2024. [Online]. Available: https://ntrs.nasa.gov/citations/19820006186

[4] T. Yasuda, K. Fukui, K. Matsuo, H. Minagawa, and R. Kurimoto, "Effect of the Reynolds Number on the Performance of a NACA0012 Wing with Leading Edge Protuberance at Low Reynolds Numbers," *Flow Turbulence Combust*, vol. 102, no. 2, pp. 435–455, Feb. 2019, doi: 10.1007/s10494-018-9978-3.

[5] V. M. Mwongera, "A review of flapping wing MAV modelling," *Int. J. Aeronaut. Sci. Aerosp. Res*, vol. 2, pp. 27–36, 2015.

[6] V. T. Gopinathan and J. B. Ralphin Rose, "Aerodynamic performance characterization of bio-inspired wings with leading edge tubercles at low Reynolds number," *Proceedings of the Institution of Mechanical Engineers, Part G: Journal of Aerospace Engineering*, vol. 237, no. 3, pp. 561–586, Mar. 2023, doi: 10.1177/09544100221103737.

[7] M. H. Masud, N.-U.-H. Naim-Ul-Hasan, A. M. E. Arefin, and M. U. Joardder, "Design modification of airfoil by integrating sinusoidal leading edge and dimpled surface," in *AIP conference proceedings*, AIP Publishing, 2017. Accessed: Oct. 31, 2024. [Online]. Available: https://pubs.aip.org/aip/acp/article-abstract/1851/1/020048/885472

[8] A. Skillen, A. Revell, J. Favier, A. Pinelli, and U. Piomelli, "Investigation of wing stall delay effect due to an undulating leading edge: An LES study," in *Eighth International Symposium on Turbulence and Shear Flow Phenomena*, Begel House Inc., 2013. Accessed: Oct. 31, 2024. [Online]. Available: https://www.dl.begellhouse.com/references/3ce1b491115b5c16,15f13bde2c0586bc,272211f67047f74c.html

[9] A. Corsini, G. Delibra, and A. G. Sheard, "On the role of leading-edge bumps in the control of stall onset in axial fan blades," *Journal of fluids engineering*, vol. 135, no. 8, p. 081104, 2013.

[10] H. Kim, J. Kim, and H. Choi, "Flow structure modifications by leading-edge tubercles on a 3D wing," *Bioinspiration & biomimetics*, vol. 13, no. 6, p. 066011, 2018.

[11] M. H. Masud, M. La Mantia, and P. Dabnichki, "Estimate of Strouhal and Reynolds numbers for swimming penguins," *Journal of Avian Biology*, vol. 2022, no. 2, p. e02886, Feb. 2022, doi: 10.1111/jav.02886.

[12] N. I. Ismail, H. Yusoff, H. Sharudin, S. Suhaimi, and S. K. Hamdan, "Lift, drag and pitching moment performances of different wing profiles for MAV wings," in *Journal of Physics: Conference Series*, IOP Publishing, 2019, p. 012024. Accessed: Nov. 21, 2024. [Online]. Available: https://iopscience.iop.org/article/10.1088/1742-6596/1349/1/012024/meta

[13] D. B. Zadorozhna, O. Benavides, J. S. Grajeda, S. F. Ramirez, and L. De La Cruz May, "A parametric study of the effect of leading edge spherical tubercle amplitudes on the aerodynamic performance of a 2D wind turbine airfoil at low Reynolds numbers using computational fluid dynamics," *Energy Reports*, vol. 7, pp. 4184–4196, Nov. 2021, doi: 10.1016/j.egyr.2021.06.093.